Liquid Crystals

Publication details, including instructions for authors and subscription information:
http://www.informaworld.com/smpp/title~content=t713926090

Effect of chirality on phase transitions in re-entrant liquid crystals

E. Gorecka; J. Mieczkowski; Li Chen

To cite this Article Gorecka, E. , Mieczkowski, J. and Chen, Li(1997) 'Effect of chirality on phase transitions in re-entrant liquid crystals', Liquid Crystals, 23: 2, 185 — 191

To link to this Article: DOI: 10.1080/026782997208433

URL: http://dx.doi.org/10.1080/026782997208433

LIQUID CRYSTALS, 1997, VOL. 23, NO. 2, 185–191

Effect of chirality on phase transitions in re-entrant liquid crystals

by E. GORECKA†*, J. MIECZKOWSKI‡ and LI CHEN§¶
†Laboratory of Dielectrics and Magnetics, Department of Chemistry,
Warsaw University, Al. Zwirki i Wigury 101, 02-089 Warsaw, Poland
‡Laboratory of Natural Compounds, Department of Chemistry,
Warsaw University, Pasteura 1, 02-093 Warsaw, Poland
§Liquid Crystal Institute, Kent State University, Kent, Ohio 44242, U.S.A.

(*Received 18 November 1996; in final form 3 February 1997; accepted 27 February 1997*)

The phase diagrams for enantiomers and their racemic counterparts have been compared in order to determine the influence of chirality on re-entrant phenomena. It has been found that chirality affects the location of the partially bilayer SmA_d and monolayer smectic SmA_1 phase areas, while the position of the smectic X phase remains nearly unchanged. This result shows that the N–SmA phase transition is influenced by a molecular chiral discrimination effect. Moreover, in enantiomeric systems, a N^*_{re1}–N^*_{re2} phase transition has been detected by DSC within the re-entrant nematic gap which is limited by the smectic A_d and the SmX phases. Based on preliminary data, the SmX phase seems to be either a weakly tilted $SmC̃$ antiphase or an incommensurate orthogonal mesophase.

1. Introduction

It is well known that molecular chirality induces a spontaneous twist of the director in the nematic (N) phase leading to a helical superstructure. On the other hand, in a smectic A phase the twist deformation is entirely expelled which causes either destabilization of the smectic phase in favour of the nematic phase [1] or formation of a highly dislocated TGB phase [2]. In the first case the temperature of the N–SmA phase transition is lower than the transition temperature in the non-twisted system in proportion to the accumulated twist energy. Within the mean field calculations, the temperature shift is $\Delta T^2 \sim K_2 q^2$, where K_2 is the twist elastic constant and q is the helix wavevector. The temperature change is expected to be rather small, $\Delta T/T \sim 10^{-2}$ and should decrease when the system exhibits critical fluctuations [1]. The phase transition can also be influenced by the molecular chiral discrimination (CD) effect [3]. Discrimination is broadly understood in terms of electrostatic and dispersive forces which cause unequal interactions within the pairs of molecules with like- and unlike-chirality. The CD is rather small for liquids, since the energy of the chiral discrimination greatly diminishes when averaged over all the mutual orientations of the molecules. The typical normalized differences between enantiomers and racemates for boiling points, refractive indices etc are of the order 10^{-4} [3]. The effect can profoundly increase in systems with orientational order of the molecules. It is known that the energies of the crystal latices, and consequently the melting points, of enantiomers and the corresponding racemates can differ significantly [3].

For our studies, we chose liquid crystals that exhibit partial orientational ordering. To diminish the influence of the twist deformation on the phase transitions, thus allowing us to observe nearly pure CD effects, materials with a re-entrant nematic phase were studied. In these systems, at the stability limit of the smectic A_d phase, the twist director modulation in the N phase must vanish as a necessary condition for the continuous transitions at the N_{re}–SmA_d–N double critical end (DCE) point. Also, around tricritical points which might exist on N_{re}–SmA_1 phase transition lines [4], the twist deformation is expected to be small. The preliminary studies showed a significant influence of the CD effect on the location of the double critical point [5]. In this communication we describe in detail the re-entrant phase diagram for highly chiral enantiomers and their racemic counterparts. We show that the positions of both smectic A areas are markedly affected by chirality. The systems studied are the first liquid crystals which clearly exhibit chiral discrimination. We have also found that additional subphases within re-entrant nematics are generated in enantiomeric compounds.

2. Experimental

The studies were performed with mesogenic phenylbutyrates, with different values of n,

---

*Author for correspondence.

¶Present address: International Forecasting, Federal Express Corporation, 2003 Corporate Avenue, Memphis TH38194, U.S.A.

0267–8292/97 $12·00

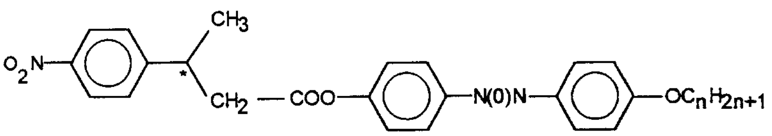

in which the asymmetric centre placed within the mesogenic core ensures a high twisting ability of the molecules. The strongly polar NO_2 group (electric dipole moment 3·8 D) was introduced into the molecular structure as a terminal group in order to develop the re-entrant phenomenon. The synthesis of the relevant compounds has already been described [6]. The ^{1}H NMR spectra (JEOL-4H-100) and IR spectra (using KBr pellets or films) for the synthesized compounds were consistent with the expected molecular structure. The optical purity of the enantiomers was controlled by checking the optical rotation of the final products, as well as of *R*-(-)-3-phenylbutyric acid and its ester with (1*R*,2*S*,5*R*)-(-)-menthol which were used in the synthesis. The phase transition temperatures were determined by DSC (DSC7 Perkin-Elmer), complemented by microscopic methods (Nikon-Optiphot2 and Mettler HP82 hot stage). The scanning rate of $5\,\mathrm{K\,min^{-1}}$ was used in the DSC studies unless slower scans were needed for better resolution. The phase identification was confirmed by X-ray studies performed with a Siemens X-1000 system equipped with a two dimensional positional sensitive area detector and graphite monochromater. The X-ray measurements were performed with powder samples.

3. Results

3.1. *Phase diagrams*

The phase transition temperatures for the pure enantiomeric compounds and their racemic counterparts are collected in the table and presented in figure 1. The mesophase identification was confirmed by X-ray measurements. In the range of chiral SmC$_d^*$ phase, typical for ferroelectric mesophases bistable electrical switching was observed; apparent tilt angle ~5°. The phase transition temperatures determined by DSC agreed with results from microscopic measurements except for the materials with a narrow nematic range. In the *R*-(-)-17 compound, in thin homeotropically aligned samples, fast cooling scans gave the phase sequence SmA$_d$–SmC$_d$–SmX without a N$_{re}$ phase on some occasions, while on fast heating the SmX–N$_{re}$–SmA$_d$ phase sequence could be observed.

The most striking difference between the corresponding phase diagrams for the enantiomers and racemates is the location of the smectic A areas. In the chiral system, both smectic A phases, the partially bilayered SmA$_d$ and monolayer SmA$_1$, are strongly destabilized, with the result that the temperature range of the re-entrant nematic phase is enhanced. Assuming the screw parabolic shape [5] for the phase boundaries $(y/y_o-1)=A(y/y_o-1)+B(x/x_o-1)^{1/2}$ where $y=T$, $x=n$ or $y=n$ and $x=T$ for the A$_d$ and A$_1$ phases, respectively; it is found that the apex of the A$_d$ area is moved from the $n_o=11{\cdot}96\pm0{\cdot}05$ $T_o=107{\cdot}5\pm0{\cdot}2$°C point in the racemic compounds, to the $n_o=12{\cdot}44\pm0{\cdot}05$ $T_o=106{\cdot}7\pm0{\cdot}2$°C point in the enantiomeric compounds. The calculated position of the critical points qualitatively agree with those experimentally determined for the binary mixtures [6, 7].

The corresponding shift of the SmA$_1$ apex is from the $n_o=11{\cdot}01\pm0{\cdot}1$ $T_o=91{\cdot}7\pm0{\cdot}2$°C to the $n_o=11{\cdot}2\pm0{\cdot}3$ $T_o=82{\cdot}6\pm0{\cdot}2$°C point. An important feature of the topologies of the phase diagrams studied is that the chirality only slightly affects the position of the other smectic phases, SmC$_d$ and SmX. As a consequence, the narrow (e.g. 3·3 K in compound (±)-15) nematic re-entrant gap separating the SmA$_1$ and SmA$_d$(C$_d$) phases in the racemic compounds (figure 1 (*b*)) significantly broadens in the enantiomers (e.g. 16·3 K in compound *R*-(-)-15) and appears either between the SmA$_1$ and SmA$_d$ phases as for compound *R*-(-)-13 or between the SmX and SmA$_d$(C$_d$) phases (compounds *R*-(-)-*n*, $17\geqslant n\geqslant 14$) (figure 1 (*a*)).

3.2. *SmX phase*

The SmX phase was detected in both enantiomeric and racemic systems for long chain homologues ($n\geqslant 14$). Its appearance is accompanied by an easily detectable enthalpy (e.g. $\Delta H=0{\cdot}26\,\mathrm{J\,g^{-1}}$ in compound *R*-(-)-15). At the SmX–N$_{re}$ phase transition on thermograms a sharp peak without noticeable pretransitional anomalies in specific heat was found (figure 4), while at the SmX–SmA$_1$(C$_d$) phase transition, pretransitional effects are detected in both SmX and SmA$_1$/C$_d$ phases (figure 3). In microscopic observations, the SmX phase appears as a faint fan texture, indicating a rather low birefringence of the phase. This type of texture has been detected when cooling a freely suspended film of the SmA$_1$ phase. At the N$_{re}$–SmX phase transition, a texture with filaments, typical for the cholesteric–smectic phase transition, was observed. Although the texture of the SmX reminds one of that observed in the chiral $\mathrm{Sm}\tilde{\mathrm{C}}^*$ antiphase [8], neither spontaneous polarization ($\mathrm{P_s}<1\,\mathrm{nc\,cm^{-2}}$) nor electrical switching was detected even with a high electric field (up to $20\,\mathrm{V\,\mu m^{-1}}$). Since

Table. Phase transition tempertures in °C and total enthalpies[a] (J g^{-1}) or heat capacity changes [J g^{-1} K^{-1}] detected by DSC on a heating scan at a rate of 5° min^{-1}. In the table, the melting point of the most stable crystal phase is given. Transition temperatures in italics are for monotropic phase transitions.

Data for the (±)-*n* racemic systems

n	Melting point	SmX	SmA$_1$	N$_{re}$	SmC$_d$	SmA$_d$	N	I
6	83·6	—	—	—	—	—	● 125·5(1·7)	●
8	87·4	—	● *73·8*(0·09)	—	—	—	● 122·0(1·7)	●
10	97·8	—	● *90·1*(0·20)	—	—	—	● 120·7(2·6)	●
11	88·0	—	● 92·0(0·13)	—	—	—	● 121·5(2·6)	●
12	73·5	—	● 92·0(0·01)	● 102·0(0·00)	—	● 112·5(0·00)	● 121·9(3·3)	●
13	71·6	● *47*	● 82·0(0·12)	● 86·1(0·15)	—	● 121·7(0·20)	● 122·1(4·3)	●
14	70·1	● *57·8*(0·19)	● 73·1(0·14)	● 77·4(0·11)	—	● 124·8(5·58)	—	●
15	74·9	● *56·0*(0·18)	● *62·9*(0·06)	● *66·2*(0·07)	● *68·2*[0·09]	● 126·0(6·52)	—	●
16	71·9	● *66·1*(0·47)	—	—	● *70·5*[0·14]	● 128·7(6·94)	—	●
17	72·7	● *66·0*(0·57)	—	—	● *69·7*[0·22]	● 129·9(7·14)	—	●

Data for the *R*-(—)-*n* enantiomeric compounds

n	Melting point	SmX	SmA$_1$	N$^*_{re1}$	N$^*_{re2}$	SmC$^*_d$	SmA$_d$	N*	Bp	I
11	81·6	—	● 82·6(0·39)	—	—	—	—	● 114·9	● 116·2(2·7[b])	●
12	76·8	—	● 79·0(0·04)	—	—	—	—	● 119·4	● 120·4(3·4[b])	●
13	71·2	—	● 72·8(0·04)	—	● 95·0(0·00)	—	● 115·7(0·05)	● 119·5	● 120·3(2·9[b])	●
14	64·9	● *55·6*(0·19)	—	● ~70	● 83·6[0·08]	—	● 123·1(5·36)	—	—	●
15	70·5	● *62·9*(0·26)	—	● *70·5*(0·12)	● 79·1[0·06]	—	● 125·7(7·3)	—	—	●
16	63·4	● 64·5(0·27)	—	● 68·1(0·50)	● 73·1(0·09)	—	● 126·1(7·35)	—	—	●
17	63·1	● 65·8(0·08)[c]	—	—	● 68·0[0·11]	● 70·0[0·20]	● 127·0(7·76)	—	—	●

[a] The total heat effects are provided without differentiating between latent enthalpy and heat capacity pretransitional changes.

[b] Enthalpy of the N–Bp–I phase transition was not resolved.

[c] For *R*-(—)-17 an additional transition SmX–SmX′ was detected at 63·8°C (0·14 J g^{-1}).

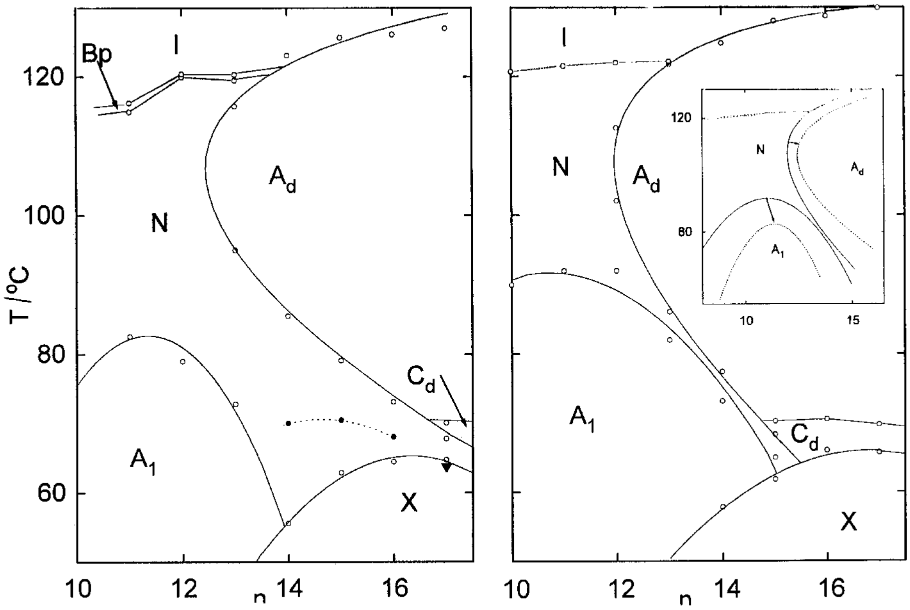

Figure 1. Phase diagram for enantiomeric (left) and racemic (right) compounds. In the inset the chirally-induced shift of the SmA_d and SmA_1 areas is indicated. Filled circles denote the N_{re1}–N_{re2} phase transition, the filled triangle denotes the SmX–SmX phase transition (see the text).

the value of the spontaneous polarization is to a first approximation related to the value of the tilt angle [9], the lack of a measurable P_s might suggest a weakly or untilted smectic structure.

X-ray measurements performed with compound *R*-(-)-16 in the temperature range of the SmX phase (figure 2) revealed two quasi-Bragg low angle reflections, corresponding to the monolayer $d/L \sim 0{\cdot}98$ and partially bilayer $d/L \sim 1{\cdot}3$ (*d* is the layer spacing, *L* is molecular length) distances, and single high angle diffuse scattering, pointing to a liquid-like molecular order within the smectic layers (figure 2). The range of the in-plane translational correlations calculated from the width of the diffuse Lorentian-type peak is similar to that detected in SmA-type phases and does not exceed 30 Å. The observed X-ray scattering pattern can be interpreted as arising from a Sm$\tilde{C}$ antiphase if the existence of an additional unresolved peak close to the direct beam is assumed. However, we cannot exclude the possibility that the SmX is an orthogonal mesophase with liquid-like in-plane order in which two collinear incommensurate density modulations coexist. Careful high resolution X-ray studies with aligned samples are necessary before incommensurability of the mesophase can be established conclusively [10, 11].

Studies of the phase transition in binary mixtures of

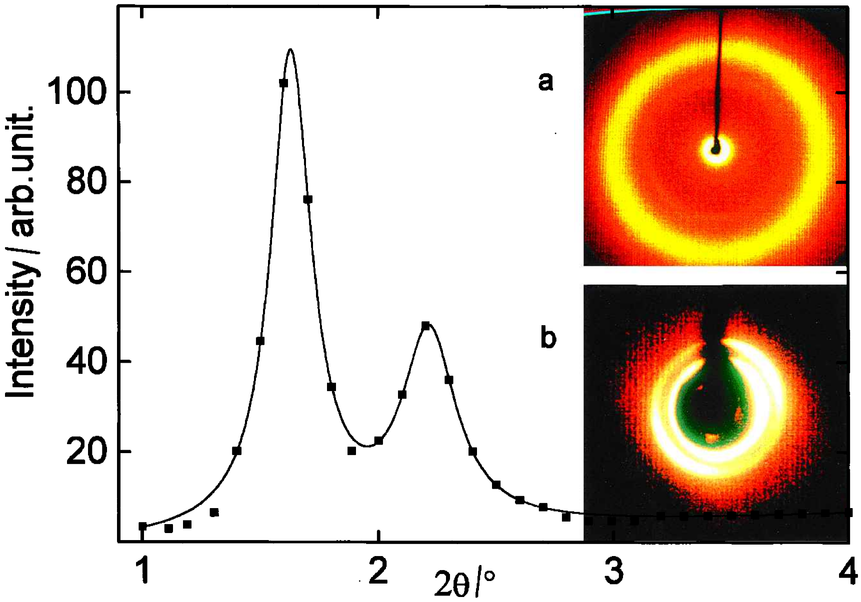

Figure 2. 2θ scan in the low angle region obtained for the powder sample of *R*-(-)-16 in the temperature range corresponding to the SmX phase. In the inset wide angle (*a*) and small angle (*b*) X-ray patterns obtained in separate runs are shown.

enantiomer *R*-(-)-17 with its racemic counterpart show the presence of an additional SmX′ subphase (figure 3). Strong destabilization of the SmX′ phase with decreasing enantiomer concentration provides evidence for the chiraly induced nature of this subphase.

3.3. N^*_{re}–N^*_{re} *phase transition*

In the enantiomeric system, an additional phase transition has been found within the temperature range of the re-entrant nematic phase. The N^*_{re1}–N^*_{re2} phase transition was observed for enantiomers $14 \leqslant n \leqslant 16$ in which the nematic gap is limited by SmA_d and smectic X phases. On thermograms, this phase transition was observed as a double peak accompanied by a heat capacity jump for two higher homologues *R*-(-)-15 and *R*-(-)-16 and as a broad bump in the *R*-(-)-14 enantiomer, where the re-entrant gap is widest (figure 4). The N^*_{re1}–N^*_{re2} phase transition is also detectable in careful microscopic observations. In homogeneously well aligned thin samples, when approaching the transition temperature a net of square defects appears. Below and above the transition temperature a texture with a few oily streaks, typical for the cholesteric phase, is observed. Although the square defects observed at the N^*_{re1}–N^*_{re2} phase transition might be parabolic defects [12, 13] caused by a small discontinuity of the helical pitch *p*, preliminary optical rotary power measurements did not reveal any noticeable anomaly at the N^*_{re1}–N^*_{re2} phase transition. Systematic helical pitch measurements at the N^*_{re1}–N^*_{re2} phase transition could not be performed since the selective reflection is in the UV range where strong molecular absorption bands appear. Tentative observations of Cano–Grandjean steps on nematic droplets gave $p \sim 0{\cdot}2\,\mu m$ and showed that the helical pitch critically increases when approaching smectic boundaries. As a result, within the re-entrant nematic gap two temperature regions of selective reflection of visible light were detected.

The small texture changes and the lack of a strong helical pitch discontinuity at the N^*_{re1}–N^*_{re2} phase transition suggest that the nematics deviate in their short range order. It might be assumed that the phase transition takes place between nematic phases with different types of fluctuations induced by the neighboring SmA_d and SmX phases. To date, the existence of two distinct re-entrant nematic phases separated by a first order transition line has been predicted [14] and recently confirmed [15] for systems with a narrow nematic gap limited by smectic A_l and A_d phases.

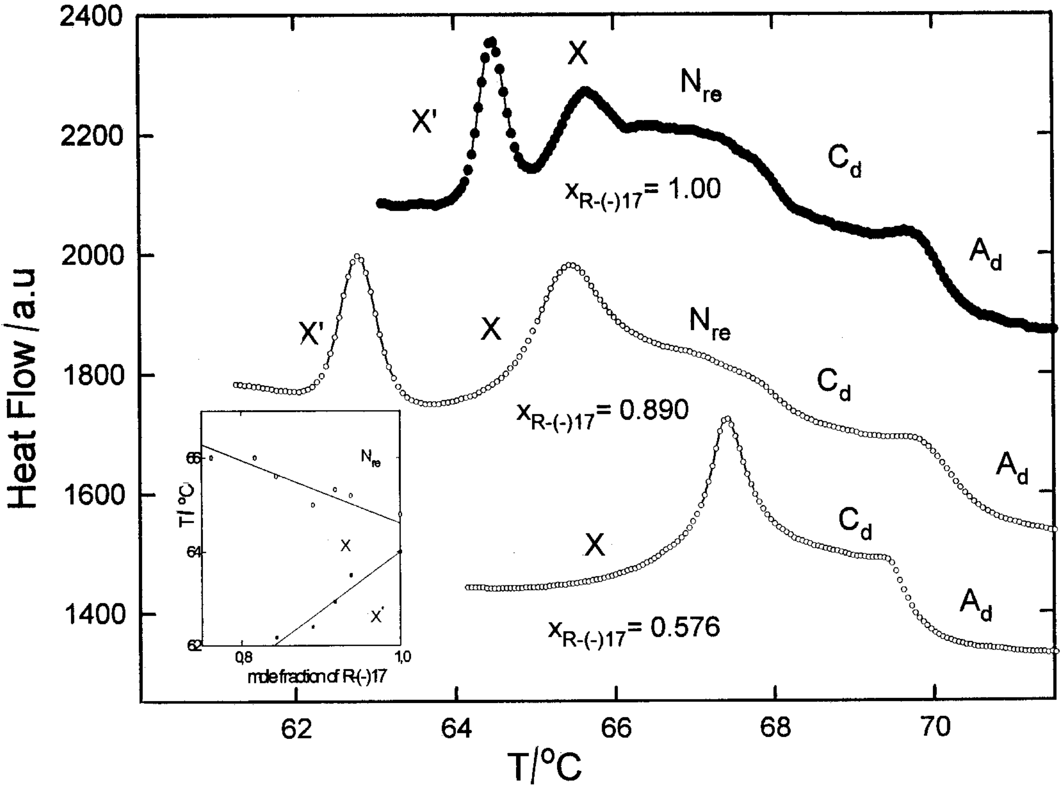

Figure 3. DSC thermograms for binary *R*-(-)-17 and (+)-17 mixtures taken at a 5 K min^{-1} scanning rate. In the inset part of the binary phase diagram is shown. Note that the SmX phase is destabilized with decreasing optical purity. The N_{re}–SmX transition points (open circles) were detected microscopically.

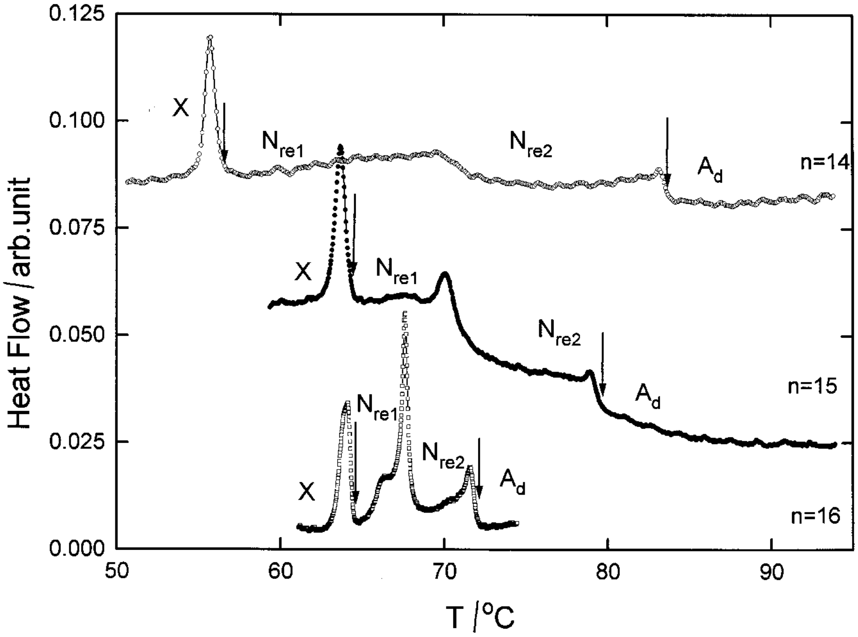

Figure 4. DSC thermograms showing SmA_d–N_{re1}–N_{re2}–SmX phase transitions in the enantiomeric homologues *R*-(-)-14, *R*-(-)-15 and *R*-(-)-16. The arrows indicate the limits of re-entrant nematic phase detected microscopically.

4. Discussion

The theory of the N–SmA phase transition predicts that in chiral systems the twist deformation destabilizes the smectic structure in favour of a nematic phase [4]. In re-entrant systems at the N_{re}–A_d–N double critical end point, helical superstructure vanishes due to the continuity of phase transition between nematic and smectic A phases at the DCE point. Thus if the twist energy is the main factor influencing the N–SmA phase transition, we could expect that the topology of the re-entrant phase diagram near the DCE point would be only weakly affected by chirality. On the contrary, experimentally it has been found that the CDE point is strongly shifted when chirality is there. The same effect is observed for the apex of the SmA_1 area. These results might indicate the influence of molecular chiral discrimination. The influence of CD on the N–SmA phase transition is pronounced near the critical points where the bulk properties are extremely sensitive to small changes in molecular interactions. The destabilization of the smectic phases shows that in the system studied, the lateral close packing in the smectic plane of molecules with unlike chirality is more efficient than the packing of like-chirality molecules. However, it should be noted that since the origin of the discriminating forces is very complex, a reverse situation involving stabilizing of the smectic phases is also possible for systems in which the chiral molecule interacts more favourably with its stereoisomeric twin than with its steromeric mirror image molecule. Thus, while the 'twist energy' always destabilizes the smectic phase, the 'chiral discrimination' effect, generally, might have a stabilizing or a destabilizing effect.

In the homologous series studied, the mesophase behaviour becomes complex when the terminal alkyl chains are extended. In both enantiomeric and racemic compounds, the smectic SmX was found for $n \geqslant 14$. Moreover in the enantiomeric compound *R*-(-)-17, the chirality generates a SmX′ subphase. It seems that both SmX and SmX′ might be either SmC antiphase type smectics or orthogonal incommensurate type mesophases with liquid-like in-plane order. Since contrary to the SmA_d and SmA_1 phases, the SmX phase is only slightly destabilized when chirality exists, the phase sequences detected in racemic compounds and their enantiomeric counterparts differ. In racemic compounds N_{re} is surrounded by SmA_1 and SmA_d/C_d phases, while in the enantiomers the N_{re} phase is also observed between SmX and SmA_d/C_d phases. In both enatiomeric and racemic compounds with the N_{re} gap limited by SmA_1 and SmA_d phases, the continuous temperature evolution of the re-entrant nematic structure is observed based on DSC studies. Different behaviour—a discontinuous change of the nematic structure—takes place if the re-entrant nematic phase is enclosed by the SmX and SmA_d phases. The N*–N* phase transition is accompanied by an easily detectable transition enthalpy, which for about a 10 K broad nematic gap, is comparable to that detected at the SmX–N* phase transition. As the range of the re-entrant nematic phase increases, the transition enthalpy diminishes, revealing a decreasing entropy difference between the nematic phases.

The synthetic part of this study is supported by UW BST-532/13/96. This work is a contribution to KBN 2P303-02407. X-ray studies were supported by a NSF ALCOM-STC project, grant no. 89-20147.

References

[1] Lubensky, T. C., 1975, *J. Phys. Colloque C1*, **36,** C1–151.

[2] Renn, S. R., and Lubensky, T., 1988, *Phys. Rev. A*, **38,** 2131; Renn, S. R., 1992, *ibid.*, **45,** 953; Goodby, J. W., Waugh, M. A., Stein, S. M., Chin, S. M., Pindak, E., and Patel, J. S., 1989, *Nature*, **337,** 449, and 1989, *J. Am. chem. Soc.*, **111,** 8119.

[3] Craig, D. P., and Mellor, D. P., 1976, in *Topics in Current Chemistry*, **63,** (Berlin: Springer-Verlag); Craig, D. P., 1979, in *Optical Activity and Chiral Discrimination*, edited by S. F. Mason (Dordrecht: Reidel); Mason, S. F., 1983, *Int. Rev. phys. Chem.*, **3,** 217; Craig, D. P., and Elsum, I. R., 1982, *Chem. Phys.*, **73,** 349; Andelman, D., 1989, *J. Am. chem. Soc.*, **111,** 6536.

[4] Raja, R., Shashidhar, R., Ratna, B. R., Heppke, G., and Bahr, Ch., 1988, *Phys. Rev. A*, **37,** 303.

[5] Leja, F., 1996, *Geometria Analityczna* (Warszawa: Panstwowe Wydawnictwo Naukowe).

[6] Pyzuk, W., Gorecka, E., and Mieczkowski, J., 1993, *Europhys. Lett.*, **22,** 371.

[7] Gorecka, E., Pyzuk, W., and Mieczkowski, J., 1994, *Mol. Cryst. liq. Cryst.*, **249,** 33.

[8] Faye, V., Babeau, A., Placin, F., Nguyen, H. T., Barois, P., Laux, V., and Isaert, N., 1996, *Liq. Cryst.*, **21,** 485.

[9] Clark, N. A., and Lagerwall, S. T., 1991, in *Ferroelectric Liquid Crystals* (Gordon and Breach Science Publishers).

[10] Ratna, B. R., Shashidhar, R., and Raja, V. N., 1985, *Phys. Rev. Lett.*, **55,** 1476.

[11] Kumar, S., Chen, Li, and Surendranath, V., 1991, *Phys. Rev. Lett.*, **67,** 322.

[12] Asher, S. A., and Pershan, P. S., 1979, *J. Phys. (Paris)*, **40,** 161.

[13] Chandrasekhar, S., 1992, *Liquid Crystals*, 2nd Edn. (Cambridge University Press).

[14] Prost, J., and Barois, P., 1984, *J. Chim. Phys.*, **80,** 65; Wang, J., and Lubensky, T., 1984, *J. Phys. (Paris)*, **45,** 1653.

[15] Nounesis, G., Kumar, S., Pfeiffer, S., Shashidhar, R., and Garland, C. W., 1994, *Phys. Rev. Lett.*, **73,** 565.